How to use online tools to generate new hypotheses for mammary gland biology research: a case study for *Wnt7b*

Yorick Bernardus Cornelis van de Grift*, Nika Heijmans*, Renée van Amerongen*^#

*Swammerdam Institute for Life Sciences, University of Amsterdam,
Science Park 904, 1098 XH Amsterdam, the Netherlands

^ corresponding author

Corresponding author e-mail: r.vanamerongen@uva.nl

Twitter: @wntlab

ORCID IDs:

YBCvdG: 0000-0003-0920-9030

NH: 0000-0002-5639-9407

RvA: 0000-0002-8808-2092

Abstract

An increasing number of '-omics' datasets, generated by labs all across the world, are becoming available. They contain a wealth of data that are largely unexplored. Not every scientist, however, will have access to the required resources and expertise to analyze such data from scratch. Luckily, a growing number of investigators is dedicating their time and effort to the development of user friendly, online applications that allow researchers to use and investigate these datasets. Here, we will illustrate the usefulness of such an approach.

Using regulation of *Wnt7b* as an example, we will highlight a selection of accessible tools and resources that are available to researchers in the area of mammary gland biology. We show how they can be used for *in silico* analyses of gene regulatory mechanisms, resulting in new hypotheses and providing leads for experimental follow up. We also call out to the mammary gland community to join forces in a coordinated effort to generate and share additional tissue-specific '-omics' datasets and thereby expand the *in silico* toolbox.

Keywords:

Wnt signaling, CTNNB1, beta-catenin, in silico analysis, *Wnt7b*, gene regulation

Introduction

The experimental technology that allows genome wide analyses at the molecular level (genomics, epigenomics, transcriptomics, metabolomics and proteomics – hereafter combinedly referred to as 'omics' approaches) continues to evolve at breathtaking speed. Despite the fact that these techniques are becoming more affordable and therefore more widely available for scientists worldwide, they are still quite expensive – a prohibitory factor for those with limited financial resources. This is especially true for sophisticated approaches such as single-cell RNA sequencing (scRNAseq) and other-single cell approaches that are still being developed. Moreover, not everyone will have local access to the required infrastructure. Of course, scientific collaborations can offer a solution. Even then, it can be a challenge to integrate a variety of these technologies into one's research program [1].

As can be gleaned from the published literature, all too frequently only a few hits or top candidates are followed up in instances where genome-wide datasets are generated. As a consequence, a wealth of data remains unexplored. These datasets constitute a rich and valuable resource for the larger scientific community. As an example, we have previously used published microarray data to identify the most stably rather than the most differentially expressed genes, resulting in a new set of reference genes for qRT-PCR studies in the developing mouse mammary gland [2].

Most 'omics' datasets are deposited in public repositories such as the NCBI Gene Expression Omnibus (https://www.ncbi.nlm.nih.gov/geo/), either in raw format or in a more processed form. While this makes them available to all scientists in theory, in practice not everyone has the bioinformatics skills and expertise to analyze these data from scratch. Fortunately, multiple labs are dedicating their time and effort to the development of online tools that allow easy and intuitive access to these datasets, allowing researchers to explore them from the comfort of their own (home) office via a user friendly graphical interface.

Here we will highlight a selection of these online tools and demonstrate how they can be used to generate hypotheses and answer biological questions in the context of mammary gland biology. To illustrate this approach, we will build a case study around *Wnt7b*, a gene that has been implicated in mammary gland development and breast cancer, but whose precise activity and mode of regulation remain unknown.

We assume that the reader is familiar with the basic principles behind the different techniques (e.g. scRNAseq, snATACseq, Hi-C), as well as with the way in which these data are commonly presented (e.g. tSNE plots). Please note that for all figures we have kept the exact style and color schemes as generated by the different online tools to aid the reader in recognizing the output when they try out these tools for themselves.

WNT7B in mammary gland development and breast cancer

WNT7B is expressed in human breast tissue and its expression has been reported to be altered in breast cancer [3,4]. Its overexpression has been associated with a poor prognosis and reduced overall survival of breast cancer patients [5]. In breast cancer, *WNT7B* has not only been shown to be expressed by the tumor cells, but also by myeloid cells present in the local microenvironment. The latter promotes angiogenesis, invasion and metastasis [6].

Its murine counterpart, *Wnt7b*, is expressed in the ductal epithelium of the mouse mammary gland [7]. The levels of *Wnt7b* remain unaltered following ovariectomy, suggesting that *Wnt7b* gene regulation is estrogen and progesterone independent [7]. During puberty, expression of *Wnt7b* is enriched in the terminal end bud epithelium, suggesting a role in branching morphogenesis [8]. *Wnt7b* has been reported to have mild transforming activities *in vitro* [9,10] and *in vivo* [11] although not all studies agree on the extent of this effect [10,12].

The precise role and regulation of *Wnt7b*/*WNT7B* in the mammary gland or breast remain unknown. So far, evidence that WNT7B protein can promote the activation of CTNNB1/TCF transcriptional complexes is lacking, despite the fact that *Wnt7b* is readily detected and shows prominent expression in luminal cells [13]. This is in contrast to other tissues, such as the skin, where the activities of WNT7B have been linked to CTNNB1/TCF driven processes [14].

Exploring spatiotemporal patterns of *Wnt7b* expression using scRNAseq data

Public scRNAseq datasets are an ideal platform to start investigating spatiotemporal gene expression in the mammary gland [15,16]. We want to highlight two user friendly scRNAseq tools that allow analysis of the *in vivo* expression patterns of a gene of interest in both the embryonic and postnatal stages of mouse mammary

gland development (Box 1). Their combined use reveals extensive details about the expression pattern of any given gene across different stages and cell populations.

Box 1: online scRNA-seq visualization tools

https://marionilab.cruk.cam.ac.uk/mammaryGland/

(Bach et al., 2017, Nature Communications [15]*)*

scRNAseq dataset that contains EPCAM+ sorted cells from multiple stages of the adult mammary gland cycle: (nulliparous (8w), gestation (14.5d), lactation (6d) and post-involution (11d). Expression of a gene of interest can be investigated in the context of an inferred cell type or developmental stage. Results are visualized as a tSNE plot and a box plot, both illustrating gene expression by cluster. Gene expression can also be displayed along the (luminal) differentiation trajectory in pseudotime.

https://tabula-muris.ds.czbiohub.org/

(The Tabula Muris Consortium, 2018, Nature [16]*)*

Large compendium of single cell transcriptome data from the model organism *Mus musculus* that contains scRNAseq datasets from 20 adult organs and tissues, including the mammary gland. This is the only online dataset available for the mammary gland that explicitly includes stromal cells and other cell types from the supportive tissue (e.g. endothelial and immune cells). Of note, all tissues have been processed and analysed by two different protocols: cells were either FACS sorted, or single-cell sorted using microfluidic droplet-capture techniques (used for fig 1) and thus sequenced using two different methodologies, providing an innate technical validation of the data when using this tool. Fat pads 2,3 and 4 were processed from virgin mice ((10-15w), and subpopulations were separated by FACS by the following markers: Basal population ($CD45^-$, $CD31^-$, $TER119^-$, $CD49f^{high-med}$, $CD29^{med-low}$), Luminal cells ($CD45^-$, $CD31^-$, $TER119^-$, $CD49f^{med-low}$, $CD24^{high-med}$), mammary repopulating cells ($CD45^-$, $CD31^-$, $TER119^-$, $CD49f^{high}$, $CD24^{med}$), and stromal cells ($CD45^-$, $CD31^-$, $TER119^-$,$CD49f^-$, $CD24^-$).

Wnt7b expression is absent (or at least below the limit of detection) in the fetal mammary gland (E18, fig1a), but emerges postnatally (fig1b,c, fig2a). Its expression is cell type specific, displaying high gene expression in the luminal compartment, and low or absent expression in basal cells and supportive tissues (fat, endothelial, immune and stromal cells) (fig1c).

Spatiotemporal expression is dynamically regulated throughout the adult mammary gland cycle (fig2a,b). In nulliparous mice, *Wnt7b* is expressed in luminal

progenitor cells, as well as in more differentiated, hormone-sensing luminal progeny (fig2b,c). During gestation and lactation *Wnt7b* expression is switched off, but it re-emerges post-involution (fig2b,c). Thus, it is exclusively expressed in the 'resting' state, be it nulliparous or post-involution. Of note, although the luminal progenitor population itself re-appears post-involution, *Wnt7b* expression is lost in this population, becoming restricted to the hormone-sensing luminal lineage post-pregnancy (fig2b,c).

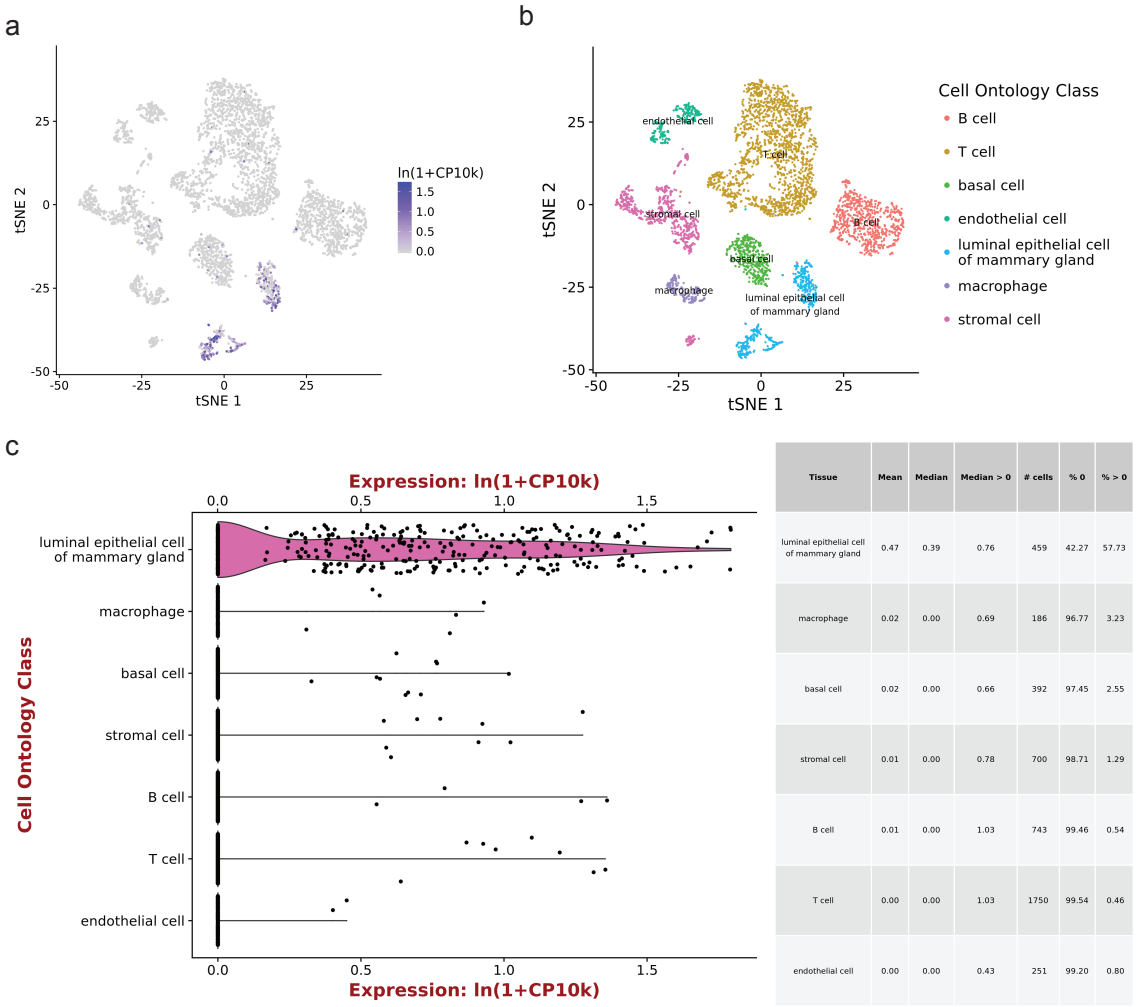

Tissue	Mean	Median	Median > 0	# cells	% 0	% > 0
luminal epithelial cell of mammary gland	0.47	0.39	0.76	459	42.27	57.73
macrophage	0.02	0.00	0.69	186	96.77	3.23
basal cell	0.02	0.00	0.66	392	97.45	2.55
stromal cell	0.01	0.00	0.78	700	98.71	1.29
B cell	0.01	0.00	1.03	743	99.46	0.54
T cell	0.00	0.00	1.03	1750	99.54	0.46
endothelial cell	0.00	0.00	0.43	251	99.20	0.80

Figure 1. Single cell RNAseq (scRNAseq) of *Wnt7b* gene expression for all cell types in the mammary gland by Tabula Muris. A) tSNE plot displaying single cell *Wnt7b* gene expression in virgin mice superimposed on pre-defined cell clusters. Gene expression is normalised to 10,000 counts per cell. B) tSNE plot defining cell ontology of the cell clusters in A). C) Violin plot of *Wnt7b* gene expression in individual cells in the clusters defined in B). Gene expression is normalised to 10.000 counts per cell. Further relevant statistical values for each subpopulation are displayed in a table format.
All plots were generated at https://tabula-muris.ds.czbiohub.org

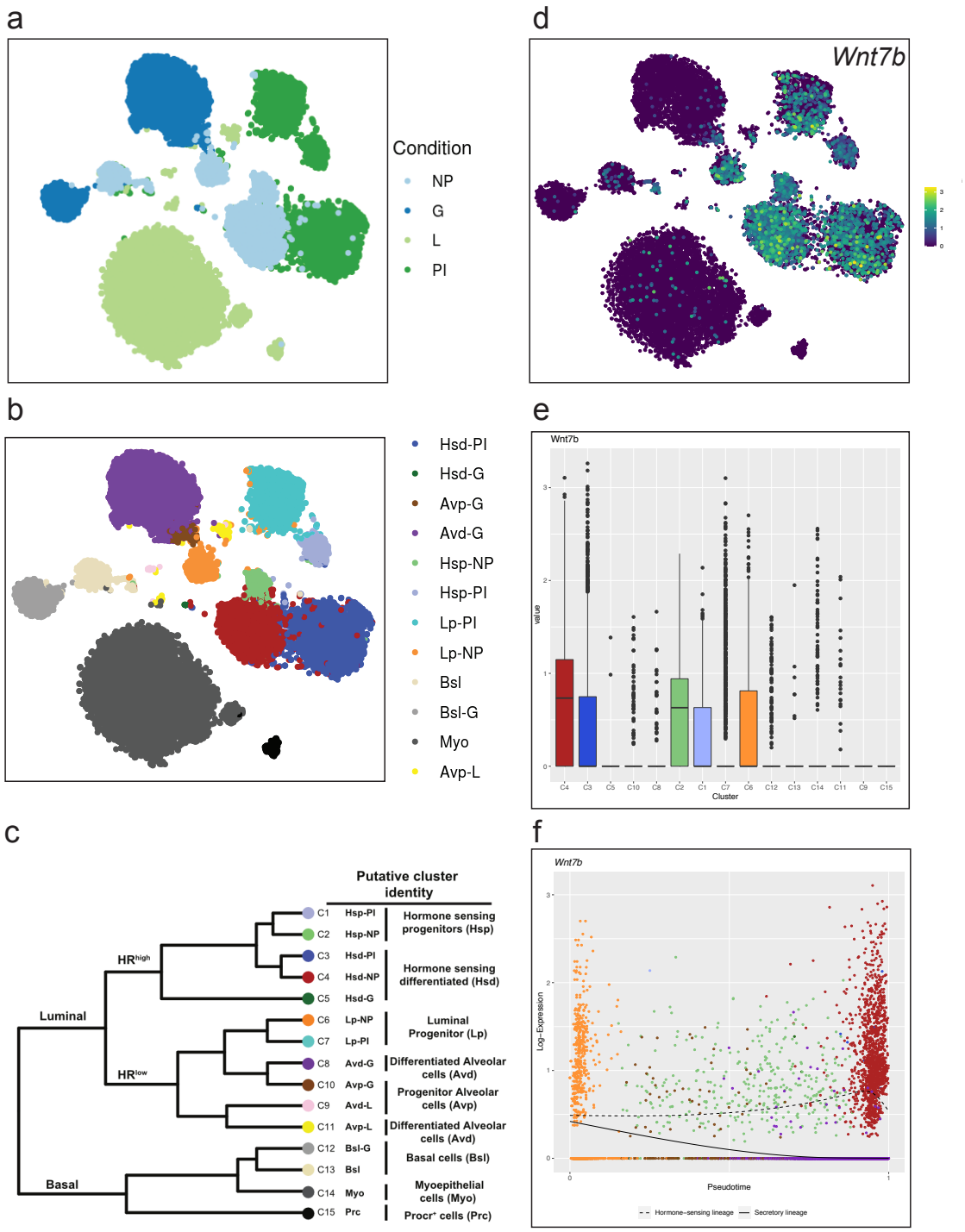

Figure 2. Single cell RNAseq (scRNAseq) of *Wnt7b* gene expression throughout mammary gland development A) tSNE plot displaying mammary gland developmental timepoints superimposed on pre-defined cell clusters. NP: Nulliparous, G: Gestation, L: Lactation, PI: Post-involution. B) tSNE plot defining cell ontology (through known marker genes) of cell clusters depicted in in A) & D). See C) for cell type classification. C) Dendrogram of clusters based on log transformed mean expression of 15 clusters. The tree was generated by Spearman's rank correlation with Ward linkage. D) tSNE plot of single cell *Wnt7b* gene log transformed mean expression superimposed on pre-defined clusters. E) Bargraphs of log transformed mean expression for each 15 clusters. F) Pseudotime trajectory of the single cell Wnt7b log transformed mean expression in the luminal lineage, displaying both the average expression in the hormone sensing and secretory lineages. Each dot represents an individual cell, and the color its associated cluster.

Plots were generated at https://marionilab.cruk.cam.ac.uk/mammaryGland/

From these analyses we would conclude that *Wnt7b* is expressed exclusively in the luminal compartment in the nulliparous mammary gland, is lost during pregnancy, and is re-established post-involution (fig3). Indeed, this is supported by other studies showing that *Wnt7b* is expressed in the virgin mammary gland, but drops at E12.5 of pregnancy to undetectable levels [7]. This underscores the validity of this approach and illustrates the usefulness of interactive *in silico* tools to determine spatiotemporal patterns of *in vivo* gene expression.

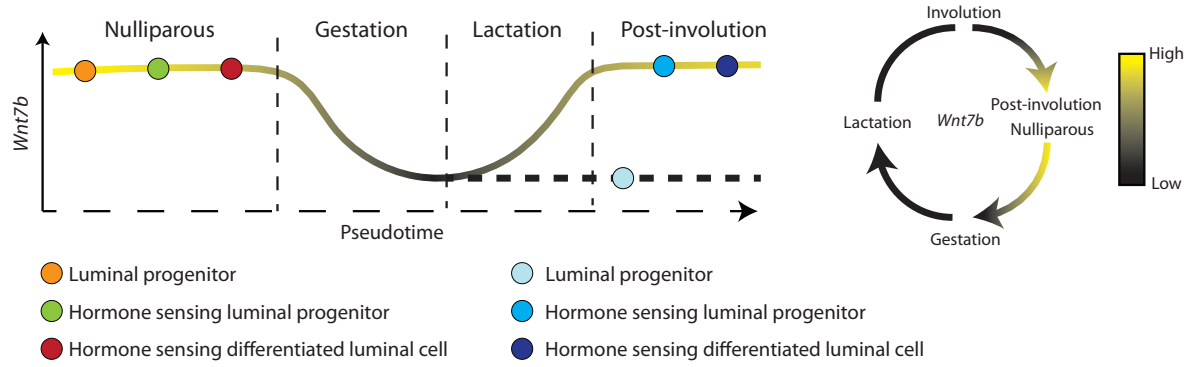

Figure 3. Graphic summary of mouse *Wnt7b* expression dynamics based on the scRNAseq data from Figure 1 and Figure 2. Drawn by the authors.

Identifying putative regulatory elements

Little is known about the molecular signals and cis-regulatory elements that control mouse *Wnt7b* or human *WNT7B* gene expression. In ER-/HER2+ breast tumors, *WNT7B* was shown to be a direct transcriptional target of the androgen receptor (AR) [17] and predicted to be regulated by Nuclear respiratory factor 1 (NRF1) [18]. Although *Wnt7b* is also expressed in hormone-responsive cells (fig2 and [13]), at present there is no experimental evidence to support that it is regulated by steroid hormones, in particular progesterone [19]. *Wnt7b* expression is not limited to the mammary gland, however. It is required for lung [20,21], and kidney development [22] to name but a few and can therefore be regulated by a myriad of signals.

One way to gain understanding into tissue-specific gene expression, is to identify cis-acting enhancer elements. Using ChIPseq analysis, a recent study predicted 440 mammary-specific super-enhancers [23]. Super-enhancers can be classified as dense clusters of transcriptional enhancers that are likely to control genes

important for cell type specification [23-25]. Only one of these was followed up in more detail in that particular study. However, a supplementary file listing all 440 of these putative regulatory elements is available. We were particularly intrigued by a sequence that spans more than 24 kb on chromosome 15 (published mm9 coordinates chr15: 85475778-85500063, mm10 coordinates chr15: 85645348-85669633), which was assigned as a putative regulator of the nearest gene: *Wnt7b* (fig4a). While it is common to do so, linear proximity alone is not an accurate measure for functional interaction between an enhancer and its putative target gene [24,25]. Other genes in this region – including two miRNAs (*Mirlet7c-2/Mirlet7b*) and a protein coding gene (*Ppara*) – might also be regulated by this particular super-enhancer. A region on the edge of this super-enhancer (mm9 coordinates chr15:85473689-85478592, published mm10 coordinates chr15: 85643259–85648162) was recently indeed associated with *Wnt7b*, albeit not in the mammary gland but in a mouse model for hair-follicle derived skin tumors, and based on strain-specific polymorphisms rather than on having been shown to directly regulate *Wnt7b* expression [14]. These results show that association of this super-enhancer with *Wnt7b* in the mammary gland is worthy of follow-up analysis.

The term “super-enhancer” is used to define a larger chromatin area that contains clusters of smaller, individual enhancers and that is enriched for active chromatin marks (e.g. H3K27ac) or occupied by transcriptional activators (e.g. MED1) and master regulatory transcription factors (e.g. STAT5A) [23,26,27]. More than 80,000 super-enhancers (combined numbers for the mouse and human genome) can be accessed through the online dbSuper database [28]. An updated version of the Super Enhancer Archive (SEA 3.0) provides another entry point [29], but this database was unfortunately offline when we were drafting this manuscript (Supplementary Table 1).

A first screen of the dbSuper database shows the tissue-specificity of super-enhancers: a putative *Wnt7b* super-enhancer has also been identified in the murine heart, lung and testis. However, this sequence does not overlap with the mammary-specific super-enhancer described by Shin et al. [23]. Instead, the dbSuper database predicts this particular location to contain two super-enhancers, identified in hair follicle stem cells, linked to *Mirlet7c-2/Mirlet7b* [30]. Additional super-enhancers in this region, identified in the kidney and the liver, are tentatively associated with *Ppara* (fig4b). It should be noted that also in dbSuper, super-enhancers and their associated genes

are linked based on a simply proximity rule to the nearest transcriptional start site (TSS) [28]. Out of the genes located in this ~500 kb area on chromosome 15, only *Atxn10* and *Wnt7b* show prominent expression in one or more mammary gland cell subpopulations, although *Ppara*, *Mirlet7c-2/b* and a non-coding RNA, *Lncppara*, may be differentially expressed at low levels (fig4c-e).

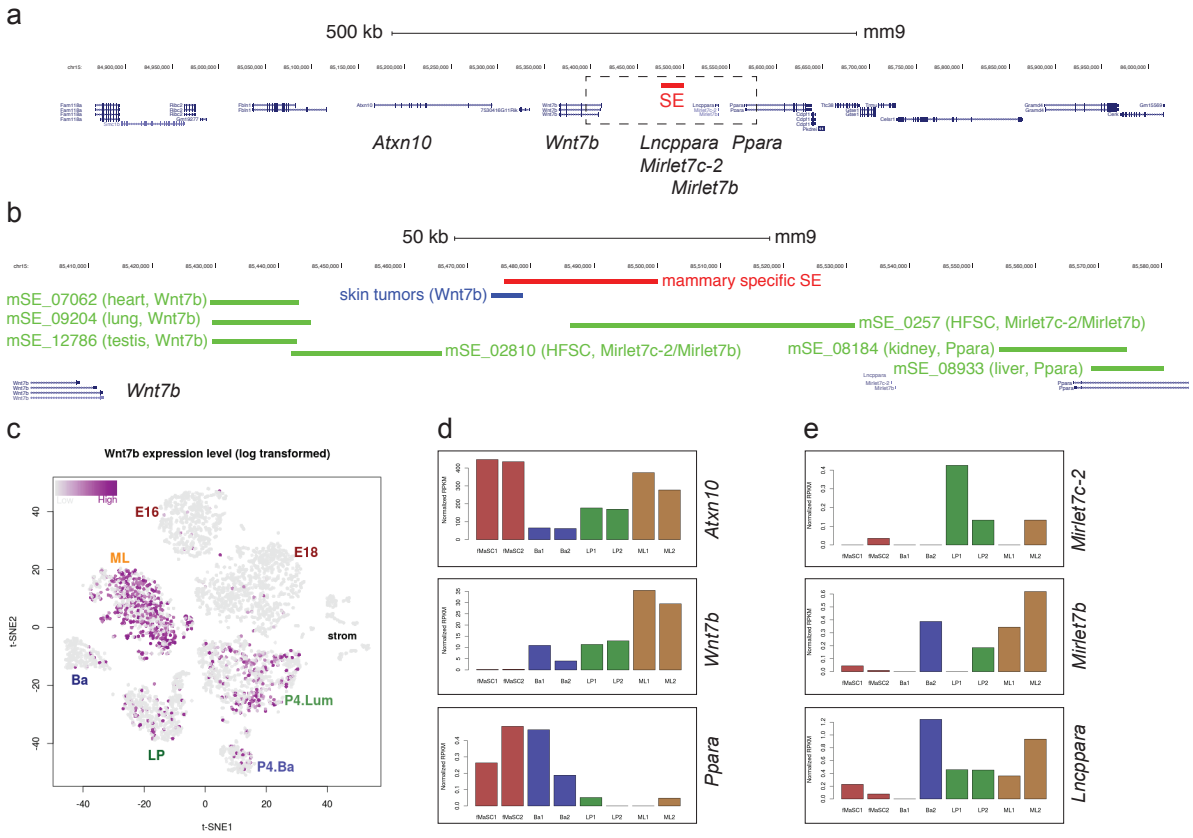

Figure 4. Overview of super-enhancers assigned to genes in the vicinity of *Wnt7b*. A) Location of a mammary-specific super-enhancer (SE, in red) on mouse chromosome 15. Scale bar is 500 kb. B) Close up of the region boxed in A. The mammary specific SE is shown in red. A *Wnt7b* associated regulatory region in skin tumors is highlighted in blue. Other super-enhancers in this genomic region, listed in Superdb, are depicted in green. The tissue of origin in which they were identified and the genes to which they have been associated based on proximity rules are indicated. HFSC= hair follicle stem cells. Scale bar is 50 kb. C) tSNE plot of single cell *Wnt7b* expression from FACS-based scRNAseq data from [31]. D) Gene expression of annotated genes in the vicinity of the mammary gland specific SE for all epithelial mammary gland subpopulations. E) Expression of putative non-coding RNAs in the vicinity of the mammary gland specific SE for all epithelial mammary gland subpopulations. D-E show normalized RPKM values. Plots for C-E were generated at https://wahl-lab-salk.shinyapps.io/Mammary_snATAC/

Determining the boundaries of the *Wnt7b* regulatory domain

In recent years, it has become generally accepted that regulatory elements control target gene expression within the confines of larger, structurally ordered regions of the chromatin known as topologically associating domains (TADs) [32].

Specific DNA sequences (i.e. regulatory elements and their target genes) are much more likely to interact within a TAD, than across a TAD boundary. A logical next step in exploring the potential regulation of *Wnt7b* by the aforementioned mammary-specific super-enhancer would therefore be to determine the boundaries of the *Wnt7b* TAD.

We used the 3D Genome Browser (Box 2) to visualize TAD predictions of the *Wnt7b* locus using publicly available Hi-C datasets [33]. In this browser, TAD boundary predictions are calculated according to the so-called directionality index, which is a method that looks at the degree of up- and downstream interaction bias for DNA regions [34]. It was noted that DNA regions at the periphery of TADs are highly biased in their direction of interaction. Upstream regions in a TAD are highly biased towards interacting with downstream regions and vice versa. Using this directional bias, the boundaries of adjacent TADs can be predicted. Their coordinates are provided by the 3D Genome Browser, which also includes an intuitive visual reference (fig5).

Box 2: Chromatin conformation capture Hi-C data

http://promoter.bx.psu.edu/hi-c/

(built by the Yue lab, described in Wang et al. (2018), The 3D Genome Browser: a web-based browser for visualizing 3D genome organization and long-range chromatin interactions [33]*)*

The 3D Genome Browser compiles published Hi-C and capture Hi-C datasets from both mouse and human cell lines or tissues, including HMEC. Chromatin conformation data from the locus of a gene or location of interest can either be displayed as a Hi-C heatmap or as a virtual 4C (with the location of interest as viewpoint). Where applicable, it will predict the boundaries of local TADs based on the provided dataset. In the upper menu bar are several options for visualizing data: In "HiC" you can visualize the data from different papers/datasets. In "Compare HiC" you can compare TADs from two different datasets. The coordinates of different TADs can also be downloaded in text file format for hg19, hg38, mm9 and mm10.

Only one mammary-specific Hi-C dataset is currently available, derived from human mammary epithelial cells (HMEC) [35]. However, TADs have been reported to be stable across cell types and even species [34,36]. Although not all TAD boundaries are equally stable [37], TAD organization can therefore also be investigated using Hi-C datasets generated from a different tissue as input.

According to this analysis, the *Wnt7b* TAD boundary lies immediately upstream of the *Wnt7b* TSS in both HMECs and mouse lymphoma cells (fig5a,b). This would imply that the mammary-specific super-enhancer identified by Shin et al. lies outside of the predicted *Wnt7b* TAD, which makes it less likely that this particular super-enhancer directly regulates the expression of *Wnt7b*. However, in other Hi-C datasets this TAD boundary is less well defined (fig5c,d).

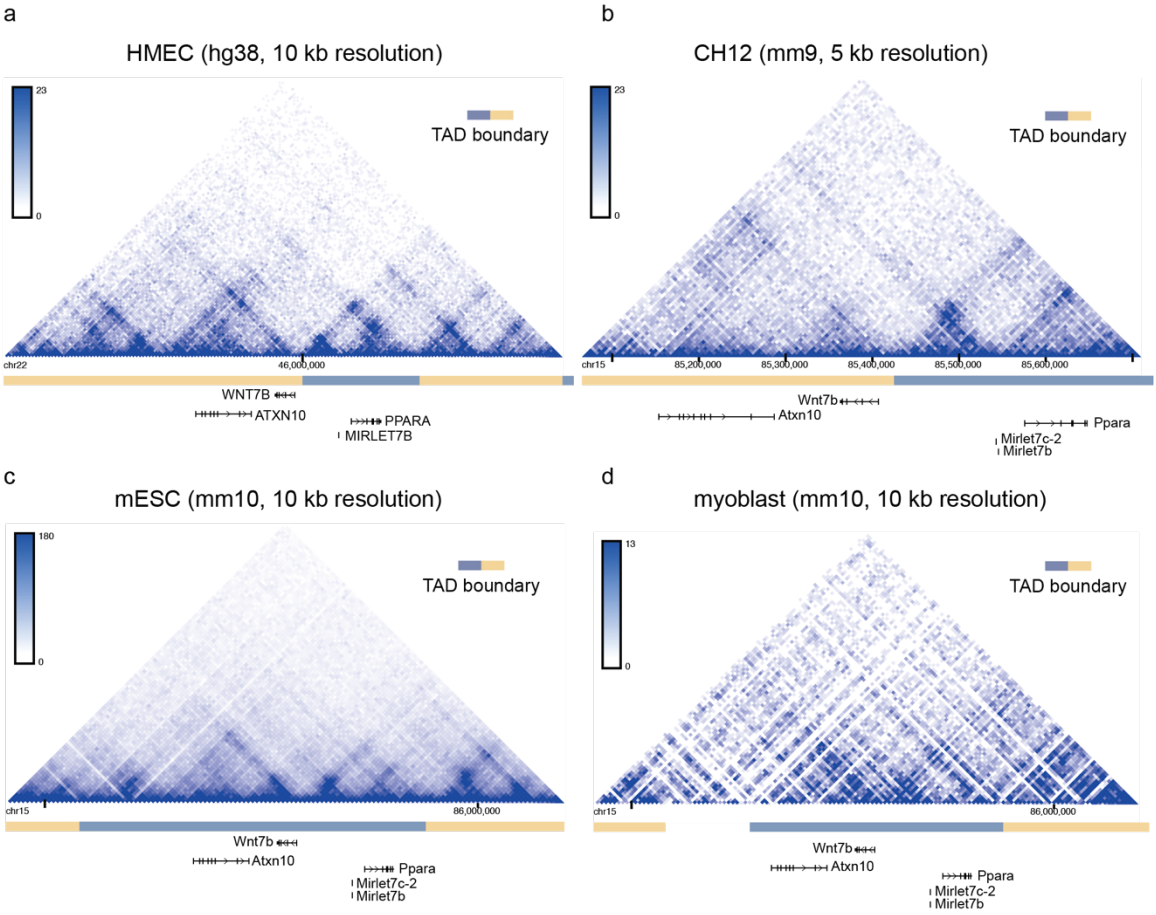

Figure 5. TAD boundary prediction using the 3D Genome Browser. In the depicted triangle, the physical interaction frequency of DNA regions is represented by the color intensity. A dark blue spot can be observed that connects the TAD boundaries of the predicted *Wnt7b* TAD, indicating that these genomic regions were found to frequently interact in this Hi-C dataset. Alternating beige and grey blocks (depicted in between the chromosome coordinates and the genes) depict individual TAD predictions. A) Hi-C data from human mammary epithelial cells, HMEC [35]. B) Hi-C data from mouse lymphoma cells, CH12 [35]. C) Hi-C data from mouse embryonic stem cells, mESC [38]. D) Hi-C data from mouse myoblasts [39]. Plots were generated at http://promoter.bx.psu.edu/hi-c/

Discovering novel regulatory interactions

To gain a better understanding of how the spatiotemporal expression of *Wnt7b* is regulated in the adult mammary gland, we can start by probing the epigenetic state

of the *Wnt7b* locus in an R shiny app published by the Wahl lab (Box 3). This tool not only allows chromatin accessibility and relevant histone modifications to be examined, but also can be used to make predictions about specific promoters and their regulatory sequences of interest. An attractive graphical interface allows intuitive interpretation of the data (fig6).

Box 3: Probing chromatin accessibility and epigenetic interactions

https://wahl-lab-salk.shinyapps.io/Mammary_snATAC/

(Chung et al., 2019, Cell Reports [40] *& Dravis et al., 2018, Cancer Cell* [41]*).*

The R shiny app published by the Wahl lab combines bulk RNAseq and H3K27 acetylation ChIPseq data from [41] with single-nucleus ATACseq (snATACseq) and scRNAseq data from [40] in an online web interface that allows its users to investigate numerous (epi)-genetic feature in fetal mammary stem cells (E18 fMaSCs), basal, luminal progenitor and mature luminal cells. This allows researchers to investigate single cell expression & chromatin state (accessibility in the case of snATACseq and active enhancer marks in the case of H3K27Ac ChIPseq) of their gene of interest, and to follow expression of the gene along a pseudotime trajectory. Moreover, if this gene is a transcription factor, its activity can be predicted for each subpopulation based on motif enrichment in open chromatin regions from snATACseq data. Lastly, based on co-accessibility of distal sites and promoter regions in single cells promoter-enhancer interactions for the gene of interest can be predicted using the so-called Cicero algorithm [42], and concurrently displayed with chromatin accessibility scores and H3K27Ac from aggregate snATACseq and bulk ChIPseq data. In the online tool, Cicero makes predictions in a region of max. 300 kb (with 150 kb upstream and 150 kb downstream of the viewpoints).

If we focus our attention on the *Wnt7b* promoter and gene region (i.e. the center portion of fig6), snATACseq reveals that the chromatin is relatively accessible in all mammary cell type subpopulations irrespective of *Wnt7b* gene expression levels (fig6, top 5 rows). In contrast, H3K27ac of the *Wnt7b* promoter and gene region is exclusively enriched in the luminal compartment (fig6, bottom 4 rows in red). This suggests that *Wnt7b* is 'primed' and open in all epithelial cells in the mammary gland, but its potential for increased gene expression is only realized in the luminal compartment where the chromatin displays the proper histone acetylation marks.

Combining the Cicero algorithm (see Box 3) with snATACseq data, this online tool can also be used to infer co-accessibility of distal sites and the promoter of their putative genes in individual cells. In this manner, Cicero can predict cis-regulatory

299 elements that would be able to interact with the *Wnt7b* promoter *in vivo*. At a co-
300 accessibility threshold of 0.15, Cicero identifies 10 regions within 150 kb up- or
301 downstream of the viewpoint that interact with the promoter of *Wnt7b*. Of these, 4 are
302 located upstream of *Wnt7b* in an area dense with H3K27ac that encompasses, but
303 extends beyond, the super-enhancer region, and 6 are located downstream of *Wnt7b*
304 (fig6).

305 The interacting regions depicted to the left of the *Wnt7b* promoter (regions 1-6,
306 located 3' distal to the TSS) all fall within in the predicted *Wnt7b* TAD (compare fig5,6).
307 These distal sites are either somewhat enriched for chromatin accessibility or
308 H3K27ac, or a combination of both epigenetic features, in adult luminal progenitor and
309 mature luminal cells compared to the adult basal subpopulation (fig6,7). The 4 regions
310 downstream of *Wnt7b* (7-10) do not display evident changes in chromatin accessibility
311 or H3K27ac when luminal cells are compared to the basal compartment, except for
312 region 8 (fig6,7). Note that the distance between region 9 and 10 spans more than 60
313 kb, which is considerably larger than the reported size of the mammary-specific super-
314 enhancer. This entire stretch of 60 kb shows characteristic marks of active and open
315 chromatin, suggesting that a much larger collection of regulatory elements may exist
316 in this area (fig6).
317
318
319
320

Next page:

Figure 6. Overview of chromatin accessibility, genomic interactions and the epigenetic status of the *Wnt7b* locus.
Top) Regions identified by Cicero as having a higher co-accessibility score than 0.15 are displayed as interacting loops with the *Wnt7b* promoter. The height of the loop indicated the corresponding Cicero score. The viewpoint size at the promoter is a stretch of 1000 bp. Middle) The 4 snATAC tracks display the aggregated snATAC signal from [40] at the *Wnt7b* locus for each epithelial mammary gland subpopulation. Ba-like: Basal-like, LP: Luminal Progenitor, ML: Mature Luminal. Bottom) The 4 H3K27 acetylation tracks display bulk ChIPseq of FACS sorted cells from [41] at the *Wnt7b* locus for each epithelial mammary gland subpopulation. ML_H3K27ac: Mature Luminal, LP_H3K27ac: Luminal Progenitor, Ba_H3K27ac: Basal, f_H3K27ac: fetal. All the data is aligned to mm10 and displayed in a window size of 300 kb. Note that *Wnt7b* is oriented in the reverse orientation (i.e. expressed from the minus strand). Regulatory regions 1-6 to the left of *Wnt7b* are therefore downstream of the promoter and regions 7-10 to the right of *Wnt7b* are upstream. Distal elements that are predicted to interact with the *Wnt7b* promoter and alter their epigenetic status in accordance to *Wnt7b* expression can have the potential to be involved in the spatial temporal regulation of Wnt7b in the mammary gland and therefore warrant further investigation. The shiny app offers an intuitive and interactive visual tool to quickly compare numerous epigenetic features, and identify novel regions of interest. It should be noted that no statistical analysis or specific coordinates are provided, although these are available in supplementary data and the GEO accession file. Hence, it serves as an excellent hypothesis generating tool that requires further validation either by *in silico* analysis or experimentation.

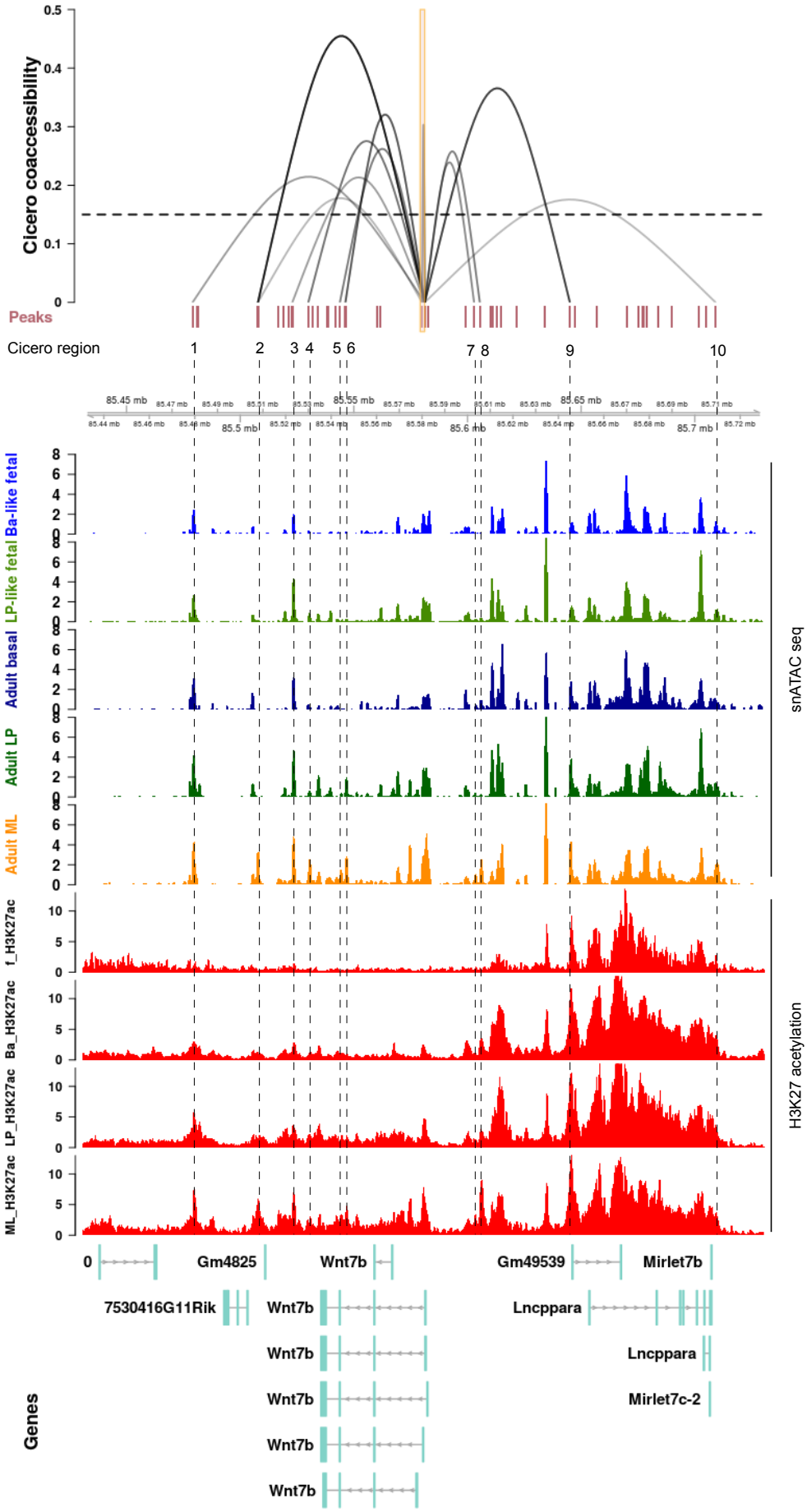

		snATAC >2				H3K27ac >5			
Region	Cicero score	Fetal	Basal	Luminal Progenitor	Mature Luminal	Fetal	Basal	Luminal Progenitor	Mature Luminal
1	> 0.2	+	+	+	+	-	-	+	+
2	> 0.4	-	-	-	+	-	-	-	+
3	> 0.2	+	+	+	+	-	-	-	+
4	> 0.25	-	-	-	+	-	-	-	-
5	> 0.25	-	-	-	-	-	-	-	-
6	> 0.3	-	-	+	+	-	-	-	-
7	> 0.2	-	-	-	-	-	-	-	-
8	> 0.25	-	-	-	+	-	-	-	+
9	> 0.35	-	+	+	+	+	+	+	+
10	> 0.15	-	-	-	+	-	-	-	-

Figure 7. Summary of the epigenetic features of each region identified by Cicero as depicted in Figure 6. Somewhat high(er) levels of snATAC seq signal are defined above a cut-off of 2 and H3K27 acetylation above a cutoff of 5. Note that the tool does not offer any statistical analysis, and therefore cut-offs were user-defined compared to the total signal in the 300 kb window. They should thus be considered reasonable, but relatively arbitrary and worthy of more in-depth investigation.

Box 4: Looking for evolutionary conservation

http://ecrbrowser.dcode.org

(Ovcharenko et al., 2004, Nucleic Acids Research [43]*).*

This web-based tool enables access to pairwise alignments for the genomes of 13 species and visualizes evolutionary conserved regions (ECRs) in a graphical interface. Users can set their own parameters to select regions with a desired cut-off (in figure 8: >85% sequence identity over >200 bp). Sequences that are conserved within these chosen parameters are represented as colored peaks. Conservation between species is shown relative to a base genome of choice (in figure 8: Hg19). Sequence information from the UCSC Genome Browser (http://genome.ucsc.edu/) [44] can be extracted when selecting the DNA region of interest.
Genome assemblies used in the ECR browser: human: Hg19, Tetraodon: tetNig1, frog: xenTro3, fugu: fr3, zebrafish: danRer7, chicken: galGal3, opossum: monDom5, rat: rn4, mouse: mm10, cow: bosTau6, dog: canFam2, chimpanzee: panTro3, rhesus macaque: rheMac2.

Exploring conservation of putative regulatory enhancer sequences

In previous studies, highly conserved sequences were associated with developmental and transcriptional regulators [45–51]. Given the fundamental role of Wnt signaling not only in vertebrate development [52], but also specifically in

mammary gland development and maintenance [53–55], focusing on conserved sequences could be another criteria for the selection of candidate *Wnt7b* enhancers. To identify conserved regions in the vicinity of *Wnt7b*, we used the evolutionary conserved region (ECR) browser (Box 4).

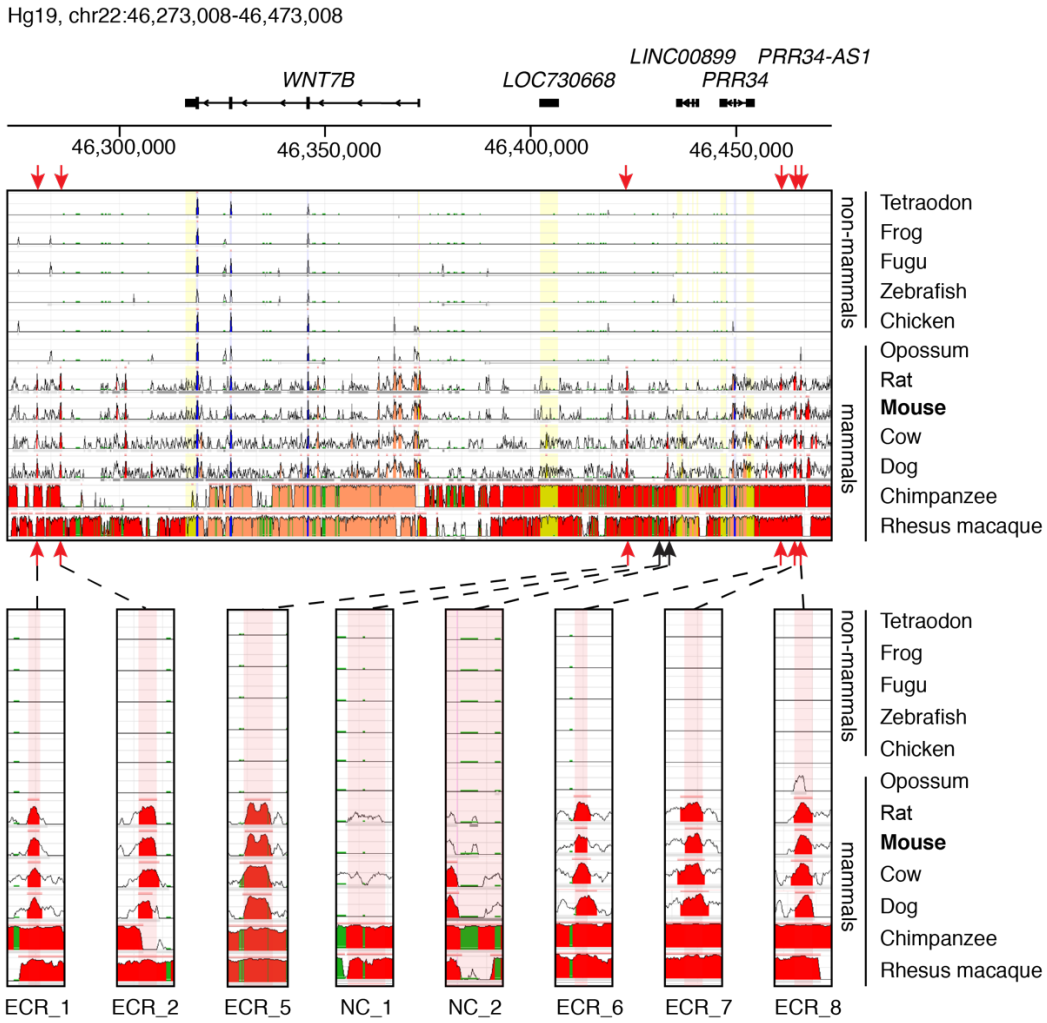

Figure 8. Selection of candidate enhancers based on sequence conservation. A 200 kb region of the human Hg19 genome assembly, 100 kb up- and downstream of *WNT7B* TSS. In each track the sequence conservation between Hg19 and one of 12 vertebrates is shown. Different colors indicate the following: Red = intergenic, salmon = intragenic, yellow = UTRs, blue = coding sequences, green = transposons and simple repeats. Locations of putative candidate *Wnt7b* enhancers are indicated by red arrows. Lower panels show zoomed in regions of 1000 bp where the candidate enhancers are located. The red shade over the tracks represent the chosen candidate enhancer region. Examples of sequences that are conserved in mammals, but not in non-mammalian vertebrates are shown (ECR_1, ECR_2, ECR_5, ECR_6, ECR_7 and ECR_8) alongside two examples of a non-conserved region (NC_1, NC_2). Parameters used: >85% sequence identity over >200 bp.

Often, conservation is scored across vertebrate species. However, in an attempt to identify regions that are specifically conserved in mammals, we specifically selected candidate sequences in a region of ~100 kb up- and downstream of the *Wnt7b* TSS that are conserved across mammalian, but not necessarily in non-mammalian vertebrate species available in the ECR browser (fig8).

353

354 **A working model for follow-up studies**

355 Of course, none of these approaches (sequence conservation, histone
356 modification, transcription factor ChIPseq), either by themselves or in combination, are
357 sufficient to definitively link any of these putative regulatory elements to *Wnt7b*. This
358 requires further experimental validation and specific follow up. However, as a
359 prediction tool these combined analyses provide an excellent starting point for
360 dissecting this super-enhancer in more detail. If we put all of the different pieces of
361 information together (fig9), we can draft some hypotheses regarding the regulation of
362 *Wnt7b* expression in the mammary gland.

363 First, we propose that in mammary epithelial cells the proposed TAD boundary
364 immediately upstream of *Wnt7b* (fig5) is not very stable, given that the Cicero
365 algorithm predicts four interactions between the *Wnt7b* promoter and regions to the
366 right of this presumed TAD boundary (i.e. regions 7-10 in fig6). Of note, two of these
367 interactions (Cicero regions 7 and 8) occur in the direct vicinity of this presumed TAD
368 boundary. The other two interactions (Cicero regions 9 and 10) border a large area of
369 active chromatin, which extends beyond the super-enhancer region previously
370 identified by Shin et al. [23]. It has not escaped our attention that this 60 kb area
371 harbors an annotated lncRNA (*Lncppara*) and two microRNAs, *MirLet7b/MirLet7c-2*,
372 which are broadly expressed and implicated in cancer formation [56–58]. Moreover,
373 this region also contains multiple conserved sequences that could represent functional
374 enhancer elements (including ECR_6, ECR_7 and ECR_8 from fig8).

375 Second, if we do take the TAD boundary prediction into account, it may be wise
376 to prioritize the interactions that occur between *Wnt7b* and more downstream
377 sequences (i.e. regions 1-6 in fig6). Although the coordinates from the Cicero
378 prediction algorithm deserve further scrutiny of the original datasets, these
379 downstream interacting regions also lie in close vicinity to conserved sequence
380 elements.

381 Third, in combination with the expression data analysis (fig1,2), the published
382 literature and the active enhancer marks (fig6,7), we can make a further prioritization
383 of putative *Wnt7b* enhancer sequences that are worthy of experimental validation and
384 follow up. In this case, region 2 is particularly interesting as is has the highest Cicero
385 score and displays both differential chromatin accessibility and H3K27 acetylation in
386 the luminal compartment.

To summarize, by using publicly available online tools we assessed the genomic conformation of the *Wnt7b* locus, and how this relates to the previously identified putative *Wnt7b* super enhancer. By examining the epigenetic status of the *Wnt7b* locus more closely, we noticed that although the *Wnt7b* promoter is predicted to interact with the super-enhancer region, this is likely not cell type specific as both chromatin accessibility and H3K27ac do not change between the basal and luminal lineages in this region. However, regions downstream of *Wnt7b* do change their epigenetic status in accordance to *Wnt7b* gene expression and are also predicted to interact with the *Wnt7b* promoter. This entire area would be worthy of experimental follow up to definitively associate specific regulatory elements with *Wnt7b* and/or other nearby genes – in particular the miRNAs and *Ppara*.

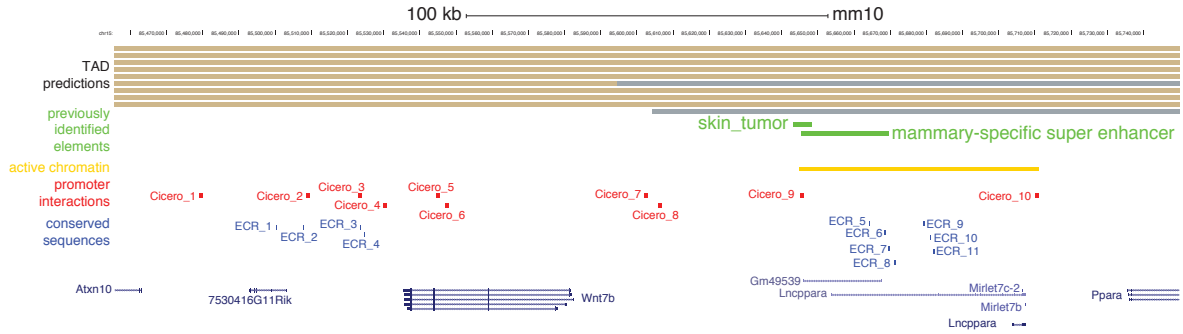

Figure 9. Integration of the insights obtained from the different analyses. Beige and grey bars at the top represent neighboring TADs as predicted in cortex (liftover from mm9), mESC (liftover from mm9), neurons (mm10), mESC (mm10), NPC (mm10), CH12 (liftover from mm9), cortical neurons (mm10), myoblast (mm10), G1E-ER4 (mm10) and HMEC (liftover from human). Previously identified (super) enhancer elements are depicted in green, the region of active chromatin identified in the Cicero analysis is depicted in yellow, promoter interactions predicted by Cicero are depicted in red and conserved sequences identified in the ECR browser are depicted in blue. Coding and non-coding genes are shown at the bottom for reference.

Discussion

Using publicly available genome wide datasets and accessible online tools, we have identified several regions that might play a role in the regulation of spatiotemporal expression of *Wnt7b* in the mouse mammary gland is regulated. Our main goal was to show the reader how these findings provide additional information for future investigations. However, we also want to use this opportunity to highlight and stress the added value of making large datasets available to a wide audience through interactive online tools. We thank our colleagues who invest their resources to do so. At the same time, we call for joint efforts from our community to ensure that the repertoire of tools as well as of accessible datasets continues to grow and remains of

high quality and value to investigators worldwide. As others have undoubtedly noticed, mammary gland and breast tissue datasets are often notoriously absent from public, large-scale -omics efforts. Generating and curating additional genome wide datasets (e.g. Hi-C and others) for both epithelial and stromal cells of multiple species, including mouse and human, would be a tremendous resource for our community as a whole. The careful generation of such datasets in combination with user-friendly online tools provide a valuable resource for researchers, and could in the long run also help to reduce animal experimentation. Certain features will enhance the user experience and promote the wide use of such tools, including the ability to export high resolution graphs (ideally allowing further customization, e.g. PDF format as offered by [15,33]) and the ability to easily download specific sequences or genome coordinates (as offered by [33,43]). Given the challenges associated with keeping these databases up to date and operating smoothly, international and consortium efforts that provide sufficient support infrastructure may, in the long term, prove to be essential in this regard.

Here we have shown how the combined use of different online tools can be applied to generate novel hypotheses. Of course, the same tools can also be used to complement existing projects by providing additional data. Ideally, in the not too near future, researchers will have a broad compendium of resources available to them that are of such high quality that they will allow *in vivo* analyses to be performed *in silico*, thereby bringing such genome-wide analyses within reach of all scientists. This will only be possible, however, if sufficient tissue-specific datasets can be accessed. Especially in the case of the mammary gland, great care should be taken to include different timepoints to cover both embryonic and postnatal developmental stages, as well as the entire gestational cycle. Here, biological and computational expertise will continually need to go hand in hand to ensure that such online tools can meet the demands of the scientific questions that are being asked.

Author contributions

Conceptualization: YBCvdG, RvA; Methodology/Experiment design: YBCvdG, NH, RvA; Investigation/Data acquisition: YBCvdG, NH, RvA; Formal analysis/Data interpretation: YBCvdG, NH, RvA; Writing – original draft: YBCvdG, NH, RvA; Writing

– revision and editing: YBCvdG, NH, RvA; Visualization: YBCvdG, NH, RvA; Supervision: RvA; Approval final manuscript: YBCvdG, NH, RvA; Project administration/Stewardship: YBCvdG, RvA; Funding acquisition: RvA.

Funding statement

This work was supported by a an NWO-ALW VIDI grant from the Dutch Research Council (864.13.002, to RvA).

Supplementary Table 1. Compilation of publicly available online tools that are outside the scope of the current case study. These tools are not specific for mammary gland biology and/or do not always include mammary gland datasets.

Tool	Description	Reference
http://asntech.org/dbsuper/index.php	dbSuper is an interactive database containing more than 80,000 putative super enhancers for 25 mouse and >100 human tissues and cell lines. The database has migrated from its original reported location (http://bioinfo.au.tsinghua.edu.cn/dbsuper/) and while functional and highly intuitive, it is not clear whether it has been updated since 2017.	[28]
http://sea.edbc.org	SEA version 3.0 was updated in 2019 and promises to be a comprehensive resource that stores predicted super-enhancers and enhancers from 11 different species and more than 200 types of cells, tissues and diseases.	[29]
https://tabula-muris-senis.ds.czbiohub.org/	A large compendium of single cell transcriptome data from the model organism *Mus musculus* that contains scRNAseq datasets of 23 organs and tissues, including the mammary gland at 6 different timepoints (1 month, 3 months, 18 months, 21 months, 24 months, 30 months). This online dataset explicitly includes stromal cells and other cell types from the supportive tissue (e.g. endothelial and immune cells). Of note, all tissues have been processed and analysed by two different protocols: cells were either FACS sorted, or single-cell sorted using microfluidic droplet-capture techniques and thus sequenced using two different methodologies, providing an innate technical validation of the data when using this tool.	[59]
https://twc-stanford.shinyapps.io/maca/	Also part of the Tabula Muris Senis effort. Offers extensive statistical analysis and visualization of bulk RNA seq datasets from 17 organs of Mus musculus at 10 different timepoints.	[60]
https://www.kobic.kr/3div/	3DIV collects human Hi-C data from 80 cells lines or tissues (including HMEC, MCF7, MCF10A) and promoter capture Hi-C from 27 tissues. Chromatin conformation data from the locus of a gene or location of interest can be either displayed as a Hi-C heatmap and as a virtual 4C (with the location of interest as viewpoint). If applicable, it also predicts the boundaries of local TADs based on the provided datasets. 3DIV offers more flexibility to its users as it allows the user to select the algorithm	[61,62]

	used to predict TADs, define the cut-off for positive interactions in the virtual 4C and it is straightforward to extract the coordinates of positive hits.	
https://www.ebi.ac.uk/gxa/sc/home	Single Cell Expression Atlas & Gene Expression Atlas: A database that compiles and visualizes published RNA & scRNA-seq datasets from Human, Mouse & a wide variety of model organisms. Selected datasets are plotted as a tSNE, and a heatmap highlighting marker genes for each annotated cluster is displayed. The database can be searched by gene across species, experiments, tissues and cell lines to reveal where this gene is expressed.	[63]
http://bioinfo.vanderbilt.edu/AE/HACER/	**HACER** is an atlas of **H**uman **AC**tive **E**nhancer to interpret **R**egulatory variants, which includes active, transcribed enhancers derived from GRO-seq, PRO-seq and CAGE data. HACER not only compiles cell type specific enhancers but also integrates transcription factor-enhancer binding prediction, validated chromatin interactions and links GWAS SNPs and eQTL variants to enhancer regions. The database includes the MCF10A and MCF7 cell lines.	[64]
https://www.spatialomics.org/SpatialDB/	An online database that compiles published spatial transcriptomic datasets and offers a web interface for spatially resolved transcriptomic data visualisation and comparison. Includes a human breast cancer dataset.	[65]
http://uofuhealth.utah.edu/huntsman/labs/spike/d3.php	tSNE visualisation of gene expression during mammary gland development: from E16 to Adult.	[31]
https://panglaodb.se/index.html	PanglaoDB is a database that collects and integrates scRNAseq data from human and mouse and presents them through an unified framework.	[66]
http://bis.zju.edu.cn/MCA/index.html#	Mouse cell atlas: A scRNAseq atlas that visualizes scRNAseq from a wide variety of mouse tissues.	[67]
https://www.cbioportal.org/	An open platform for exploring multidimensional cancer genomics data, including breast cancer. Allows you to search for mutations, CNV etc. of your gene of interest and compare this between sets.	[68,69]
http://www.enhanceratlas.org/indexv2.php	The database provides enhancer annotation in nine species, including human (hg19), mouse (mm9), fly (dm3), worm (ce10), zebrafish (danRer10), rat (rn5), yeast (sacCer3), chicken (galGal4), and boar	[70,71]

	(susScr3). The consensus enhancers were predicted based on multiple high throughput experimental datasets (e.g. histone modification, CAGE, GRO-seq, transcription factor binding and DHS). This database includes the HMEC cell line.	
https://apps.kaessmannlab.org/evodevoapp/	A database visualized by an intuitive shiny app that allows for an interactive exploration of gene expression profiles across tissues, developmental stages and species. This does not only include protein coding genes but also putative LncRNAs. The mammary gland is not included in this dataset.	[72,73]

455

References

1. Misra BB, Langefeld C, Olivier M, Cox LA. Integrated omics: tools, advances and future approaches. J Mol Endocrinol [Internet]. 2019 [cited 2020 Jul 23];R21–45. Available from: https://jme.bioscientifica.com/view/journals/jme/62/1/JME-18-0055.xml

2. Van De Moosdijk AAA, Van Amerongen R. Identification of reliable reference genes for qRT-PCR studies of the developing mouse mammary gland. Sci Rep [Internet]. 2016;6:35595. Available from: http://www.nature.com/articles/srep35595

3. Huguet EL, McMahon JA, McMahon AP, Bicknell R, Harris AL. Differential Expression of Human Wnt Genes 2, 3, 4, and 7B in Human Breast Cell Lines and Normal and Disease States of Human Breast Tissue. Cancer Res. 1994;54:2615–21.

4. Milovanovic T, Planutis K, Nguyen A, Marsh JL, Lin F, Hope C, et al. Expression of Wnt genes and frizzled 1 and 2 receptors in normal breast epithelium and infiltrating breast carcinoma. Int J Oncol. 2004;25:1337–42.

5. Chen J, Liu T-Y, Peng H-T, Wu Y-Q, Zhang L-L, Lin X-H, et al. Up-regulation of Wnt7b rather than Wnt1, Wnt7a, and Wnt9a indicates poor prognosis in breast cancer. Int J Clin Exp Pathol. 2018;11:4552–61.

6. Yeo EJ, Cassetta L, Qian BZ, Lewkowich I, Li JF, Stefater JA, et al. Myeloid wnt7b mediates the angiogenic switch and metastasis in breast cancer. Cancer Res. 2014;74:2962–73.

7. Weber-Hall SJ, Phippard DJ, Niemeyer CC, Dale TC. Developmental and hormonal regulation of Wnt gene expression in the mouse mammary gland. Differentiation [Internet]. Elsevier; 1994 [cited 2020 Jul 7];57:205–14. Available from: https://www.sciencedirect.com/science/article/pii/S0301468111601618?via%3Dihub

8. Kouros-Mehr H, Werb Z. Candidate regulators of mammary branching morphogenesis identified by genome-wide transcript analysis. Dev Dyn. 2006;

9. Wong GT, Gavin BJ, McMahon AP. Differential transformation of mammary epithelial cells by Wnt genes. Mol Cell Biol. 1994;

10. Naylor S, Smalley MJ, Robertson D, Gusterson BA, Edwards PAW, Dale TC. Retroviral expression of Wnt-1 and Wnt-7b produces different effects in mouse mammary epithelium. J Cell Sci [Internet]. 2000 [cited 2020 Jul 7];113:2129–38. Available from: http://www.stanford.edu/approx.

488 11. Roarty K, Shore AN, Creighton CJ, Rosen JM. Ror2 regulates branching, differentiation,
489 and actincytoskeletal dynamics within the mammary epithelium. J Cell Biol [Internet].
490 2015;208:351–66. Available from: http://www.jcb.org/lookup/doi/10.1083/jcb.201408058

491 12. Shimizu H, Julius MA, Giarré M, Zheng Z, Brown AMC, Kitajewski J. Transformation by
492 wnt family proteins correlates with regulation of β- catenin. Cell Growth Differ. 1997;

493 13. Cai C, Yu QC, Jiang W, Liu W, Song W, Yu H, et al. R-spondin1 is a novel hormone
494 mediator for mammary stem cell self-renewal. Genes Dev. 2014;

495 14. Krimpenfort P, Snoek M, Lambooij JP, Song JY, van der Weide R, Bhaskaran R, et al. A
496 natural WNT signaling variant potently synergizes with Cdkn2ab loss in skin carcinogenesis.
497 Nat Commun. 2019;

498 15. Bach K, Pensa S, Grzelak M, Hadfield J, Adams DJ, Marioni JC, et al. Differentiation
499 dynamics of mammary epithelial cells revealed by single-cell RNA sequencing. Nat
500 Commun. 2017;

501 16. Schaum N, Karkanias J, Neff NF, May AP, Quake SR, Wyss-Coray T, et al. Single-cell
502 transcriptomics of 20 mouse organs creates a Tabula Muris. Nature. 2018;

503 17. Ni M, Chen Y, Lim E, Wimberly H, Bailey STT, Imai Y, et al. Targeting Androgen
504 Receptor in Estrogen Receptor-Negative Breast Cancer. Cancer Cell [Internet]. Cell Press;
505 2011 [cited 2020 Jul 7];20:119–31. Available from:
506 https://www.sciencedirect.com/science/article/pii/S1535610811001966?via%3Dihub#fig3

507 18. Ramos J, Das J, Felty Q, Yoo C, Poppiti R, Murrell D, et al. NRF1 motif sequence-
508 enriched genes involved in ER/PR −ve HER2 +ve breast cancer signaling pathways. Breast
509 Cancer Res Treat. 2018;

510 19. Fernandez-Valdivia R, Mukherjee A, Creighton CJ, Buser AC, DeMayo FJ, Edwards DP,
511 et al. Transcriptional response of the murine mammary gland to acute progesterone
512 exposure. Endocrinology. 2008;

513 20. Shu W, Jiang YQ, Lu MM, Morrisey EE. Wnt7b regulates mesenchymal proliferation and
514 vascular development in the lung. Development. 2002;

515 21. Rajagopal J, Carroll TJ, Guseh JS, Bores SA, Blank LJ, Anderson WJ, et al. Wnt7b
516 stimulates embryonic lung growth by coordinately increasing the replication of epithelium
517 and mesenchyme. Development. 2008;

518 22. Yu J, Carroll TJ, Rajagopal J, Kobayashi A, Ren Q, McMahon AP. A Wnt7b-dependent
519 pathway regulates the orientation of epithelial cell division and establishes the cortico-

520 medullary axis of the mammalian kidney. Development. 2009;

521 23. Shin HY, Willi M, Yoo KH, Zeng X, Wang C, Metser G, et al. Hierarchy within the
522 mammary STAT5-driven Wap super-enhancer. Nat Genet. 2016;

523 24. Dowen JM, Fan ZP, Hnisz D, Ren G, Abraham BJ, Zhang LN, et al. Control of cell
524 identity genes occurs in insulated neighborhoods in mammalian chromosomes. Cell. 2014;

525 25. Novo CL, Javierre BM, Cairns J, Segonds-Pichon A, Wingett SW, Freire-Pritchett P, et
526 al. Long-Range Enhancer Interactions Are Prevalent in Mouse Embryonic Stem Cells and
527 Are Reorganized upon Pluripotent State Transition. Cell Rep. 2018;

528 26. Whyte WA, Orlando DA, Hnisz D, Abraham BJ, Lin CY, Kagey MH, et al. Master
529 transcription factors and mediator establish super-enhancers at key cell identity genes. Cell.
530 2013;

531 27. Pott S, Lieb JD. What are super-enhancers? Nat. Genet. 2015.

532 28. Khan A, Zhang X. DbSUPER: A database of Super-enhancers in mouse and human
533 genome. Nucleic Acids Res [Internet]. 2016 [cited 2020 Jul 25];44:D164–71. Available from:
534 http://bioinfo.au.

535 29. Chen C, Zhou D, Gu Y, Wang C, Zhang M, Lin X, et al. SEA version 3.0: a
536 comprehensive extension and update of the Super-Enhancer archive. Nucleic Acids Res
537 [Internet]. 2020 [cited 2020 Jul 25];48. Available from: https://academic.oup.com/nar/article-
538 abstract/48/D1/D198/5610346

539 30. Adam RC, Yang H, Rockowitz S, Larsen SB, Nikolova M, Oristian DS, et al. Pioneer
540 factors govern super-enhancer dynamics in stem cell plasticity and lineage choice. Nature.
541 2015;

542 31. Giraddi RR, Chung C-Y, Heinz RE, Perou CM, Wahl GM, Spike BT. Single-Cell
543 Transcriptomes Distinguish Stem Cell State Changes and Lineage Specification Programs in
544 Early Mammary Gland Development. CellReports [Internet]. 2018 [cited 2020 Jul
545 15];24:1653-1666.e7. Available from: https://doi.org/10.1016/j.celrep.2018.07.025

546 32. Lupiáñez DG, Kraft K, Heinrich V, Krawitz P, Brancati F, Klopocki E, et al. Disruptions of
547 topological chromatin domains cause pathogenic rewiring of gene-enhancer interactions.
548 Cell [Internet]. 2015;161:1012–25. Available from:
549 http://www.ncbi.nlm.nih.gov/pubmed/25959774

550 33. Wang Y, Song F, Zhang B, Zhang L, Xu J, Kuang D, et al. The 3D Genome Browser: A
551 web-based browser for visualizing 3D genome organization and long-range chromatin

552 interactions. Genome Biol. Genome Biology; 2018;19:1–12.

553 34. Dixon JR, Selvaraj S, Yue F, Kim A, Li Y, Shen Y, et al. Topological domains in
554 mammalian genomes identified by analysis of chromatin interactions. Nature. Nature
555 Publishing Group; 2012;485:376–80.

556 35. Rao SSP, Huntley MH, Durand NC, Stamenova EK, Bochkov ID, Robinson JT, et al. A
557 3D map of the human genome at kilobase resolution reveals principles of chromatin looping.
558 Cell. Elsevier Inc.; 2014;159:1665–80.

559 36. Krefting J, Andrade-Navarro MA, Ibn-Salem J. Evolutionary stability of topologically
560 associating domains is associated with conserved gene regulation. BMC Biol. 2018;

561 37. McArthur E, Capra JA. Topologically associating domain (TAD) boundaries stable across
562 diverse cell types are evolutionarily constrained and enriched for heritability. bioRxiv. 2020;

563 38. Bonev B, Mendelson Cohen N, Szabo Q, Fritsch L, Papadopoulos GL, Lubling Y, et al.
564 Multiscale 3D Genome Rewiring during Mouse Neural Development. Cell. 2017;

565 39. Doynova MD, Markworth JF, Cameron-Smith D, Vickers MH, O'Sullivan JM. Linkages
566 between changes in the 3D organization of the genome and transcription during myotube
567 differentiation in vitro. Skelet Muscle. 2017;

568 40. Chung CY, Ma Z, Dravis C, Preissl S, Poirion O, Luna G, et al. Single-Cell Chromatin
569 Analysis of Mammary Gland Development Reveals Cell-State Transcriptional Regulators
570 and Lineage Relationships. Cell Rep. 2019;

571 41. Dravis C, Chung CY, Lytle NK, Herrera-Valdez J, Luna G, Trejo CL, et al. Epigenetic and
572 Transcriptomic Profiling of Mammary Gland Development and Tumor Models Disclose
573 Regulators of Cell State Plasticity. Cancer Cell. 2018;

574 42. Pliner HA, Packer JS, McFaline-Figueroa JL, Cusanovich DA, Daza RM, Aghamirzaie D,
575 et al. Cicero Predicts cis-Regulatory DNA Interactions from Single-Cell Chromatin
576 Accessibility Data. Mol Cell. 2018;

577 43. Ovcharenko I, Nobrega MA, Loots GG, Stubbs L. ECR Browser: A tool for visualizing
578 and accessing data from comparisons of multiple vertebrate genomes. Nucleic Acids Res
579 [Internet]. 2004;32:280–6. Available from: https://academic.oup.com/nar/article-
580 lookup/doi/10.1093/nar/gkh355

581 44. James Kent W, Sugnet CW, Furey TS, Roskin KM, Pringle TH, Zahler AM, et al. The
582 human genome browser at UCSC. Genome Res. 2002;12:996–1006.

583 45. Ahituv N, Prabhakar S, Poulin F, Rubin EM, Couronne O. Mapping cis-regulatory

584 domains in the human genome using multi-species conservation of synteny. Hum Mol
585 Genet. 2005;14:3057–63.

586 46. Boffelli D, Nobrega MA, Rubin EM. Comparative genomics at the vertebrate extremes.
587 Nat Rev Genet. 2004;5:456–65.

588 47. Woolfe A, Goodson M, Goode DK, Snell P, McEwen GK, Vavouri T, et al. Highly
589 conserved non-coding sequences are associated with vertebrate development. PLoS Biol.
590 2005;3.

591 48. Bejerano G, Kent WJ, Haussler D, Pheasant M, Makunin I, Stephen S, et al.
592 Ultraconserved elements in the human genome. Science (80-). 2004;304:1321–5.

593 49. Pennacchio LA, Ahituv N, Moses AM, Prabhakar S, Nobrega MA, Shoukry M, et al. In
594 vivo enhancer analysis of human conserved non-coding sequences. Nature. 2006;444:499–
595 502.

596 50. Plessy C, Dickmeis T, Chalmel F, Strahle U. Enhancer sequence conservation between
597 vertebrates is favoured in developmental regulator genes. Trends Genet. 2005;21:203–7.

598 51. Ahituv N, Rubin EM, Nobrega MA. Exploiting human - Fish genome comparisons for
599 deciphering gene regulation. Hum Mol Genet. 2004;13:261–6.

600 52. Clevers H. Wnt/β-Catenin Signaling in Development and Disease. Cell. 2006;127:469–
601 80.

602 53. Roarty K, Rosen JM. Wnt and mammary stem cells: Hormones cannot fly wingless. Curr
603 Opin Pharmacol. Elsevier Ltd; 2010;10:643–9.

604 54. Wend P, Holland JD, Ziebold U, Birchmeier W. Wnt signaling in stem and cancer stem
605 cells. Semin Cell Dev Biol. Elsevier Ltd; 2010;21:855–63.

606 55. Incassati A, Chandramouli A, Eelkema R, Cowin P. Key signaling nodes in mammary
607 gland development and cancer: β-catenin. Breast Cancer Res. 2010;12:1–14.

608 56. Sauvageau M, Goff LA, Lodato S, Bonev B, Groff AF, Gerhardinger C, et al. Multiple
609 knockout mouse models reveal lincRNAs are required for life and brain development. Elife.
610 2013;

611 57. Lai KMV, Gong G, Atanasio A, Rojas J, Quispe J, Posca J, et al. Diverse phenotypes
612 and specific transcription patterns in twenty mouse lines with ablated lincRNAs. PLoS One.
613 2015;

614 58. Madison BB, Jeganathan AN, Mizuno R, Winslow MM, Castells A, Cuatrecasas M, et al.

615 Let-7 Represses Carcinogenesis and a Stem Cell Phenotype in the Intestine via Regulation
616 of Hmga2. PLoS Genet. 2015;

617 59. Almanzar N, Antony J, Baghel AS, Bakerman I, Bansal I, Barres BA, et al. A single-cell
618 transcriptomic atlas characterizes ageing tissues in the mouse. Nature. 2020;

619 60. Schaum N, Lehallier B, Hahn O, Hosseinzadeh S, Lee SE, Sit R, et al. The murine
620 transcriptome reveals global aging nodes with organ-specific phase and amplitude. bioRxiv.
621 2019;

622 61. Yang D, Jang I, Choi J, Kim MS, Lee AJ, Kim H, et al. 3DIV: A 3D-genome Interaction
623 Viewer and database. Nucleic Acids Res. 2018;

624 62. Jung I, Schmitt A, Diao Y, Lee AJ, Liu T, Yang D, et al. A compendium of promoter-
625 centered long-range chromatin interactions in the human genome. Nat Genet. 2019;

626 63. Papatheodorou I, Moreno P, Manning J, Fuentes AMP, George N, Fexova S, et al.
627 Expression Atlas update: From tissues to single cells. Nucleic Acids Res. 2020;

628 64. Wang J, Dai X, Berry LD, Cogan JD, Liu Q, Shyr Y. HACER: An atlas of human active
629 enhancers to interpret regulatory variants. Nucleic Acids Res. 2019;

630 65. Fan Z, Chen R, Chen X. SpatialDB: A database for spatially resolved transcriptomes.
631 Nucleic Acids Res. 2020;

632 66. Franzén O, Gan LM, Björkegren JLM. PanglaoDB: A web server for exploration of
633 mouse and human single-cell RNA sequencing data. Database. 2019;

634 67. Han X, Wang R, Zhou Y, Fei L, Sun H, Lai S, et al. Mapping the Mouse Cell Atlas by
635 Microwell-Seq. Cell. 2018;

636 68. Cerami E, Gao J, Dogrusoz U, Gross BE, Sumer SO, Aksoy BA, et al. The cBio Cancer
637 Genomics Portal: An open platform for exploring multidimensional cancer genomics data.
638 Cancer Discov. 2012;

639 69. Gao J, Aksoy BA, Dogrusoz U, Dresdner G, Gross B, Sumer SO, et al. Integrative
640 analysis of complex cancer genomics and clinical profiles using the cBioPortal. Sci Signal.
641 2013;

642 70. Gao T, He B, Liu S, Zhu H, Tan K, Qian J. EnhancerAtlas: A resource for enhancer
643 annotation and analysis in 105 human cell/tissue types. Bioinformatics. 2016;

644 71. Gao T, Qian J. EnhancerAtlas 2.0: An updated resource with enhancer annotation in 586
645 tissue/cell types across nine species. Nucleic Acids Res. 2020;

646 72. Cardoso-Moreira M, Halbert J, Valloton D, Velten B, Chen C, Shao Y, et al. Gene
647 expression across mammalian organ development. Nature. 2019;

648 73. Sarropoulos I, Marin R, Cardoso-Moreira M, Kaessmann H. Developmental dynamics of
649 lncRNAs across mammalian organs and species. Nature. 2019;

650

651